

# Direct stress–strain representation for coated woven fabrics

B.N. Bridgens, P.D. Gosling \*

*School of Civil Engineering and Geosciences, University of Newcastle-upon-tyne, Newcastle-upon-tyne, NE1 7RU, UK  
Arup, 13 Fitzroy Street, London W1T 4BQ, UK*

Received 5 December 2002; accepted 26 July 2003  
Available online 3 August 2004

## Abstract

An understanding of the complex behaviour of coated woven fabrics is vital for the design of state-of-the-art fabric structures. Fabric behaviour is typically defined using elastic constants based on plane stress assumptions. This paper considers two new methods of representing fabric response: (i) use of spline functions to define response surfaces, (ii) use of stress–strain mean and difference functions (proposed by Day [IASS symposium proceedings: shells, membranes and space frames 2 (1986) 17]). Both techniques provide direct correlation between stresses and strains, eliminating the assumption of plane stress. Extensive biaxial fabric testing is proposed to assess the validity of these approaches and extend their use.

© 2004 Civil-Comp Ltd. and Elsevier Ltd. All rights reserved.

*Keywords:* Coated woven fabrics; Lightweight structures; Material models; Response surface; Biaxial behaviour; Splines; Non-linear

## 1. Introduction

Coated woven fabrics are used in a wide range of structural applications to provide lightweight, architecturally striking solutions. The design of fabric structures is complicated by the complex response of coated woven fabrics to biaxial loads in the plane of the fabric. A better understanding of the behaviour of architectural fabrics may significantly reduce levels of uncertainty in the design process and enable more ambitious architectural forms to be generated.

There are two principal types of coated woven fabric: glass fibre fabric with a PTFE (polytetrafluoroethylene) coating and polyester fabric with a PVC (poly vinyl chloride) coating. Both fabrics are composed of an open weave mesh of orthogonal yarns with a coating which encloses the mesh on both sides. The characteristics of the two fabrics are different, but the underlying deformation mechanisms are very similar. Fabric structures resist environmental loads as tensile stresses in the plane of the fabric. Under biaxial tensile loading the behaviour of coated woven fabrics is highly non-linear [1–3]. Geometric non-linearity occurs in the yarns (due to the complex twisted fibre structure) and in the finished fabric (interaction of orthogonal warp and weft yarns under biaxial in-plane stress leads to fundamental non-linearities, compounded by the effect of the coating). Material non-linearity is evident in the load–extension characteristics of both the yarn fibres and the fabric coating. The material response is also time-dependent and hysteretic

\* Corresponding author. Address: School of Civil Engineering and Geosciences, University of Newcastle-upon-tyne, Newcastle-upon-tyne, NE1 7RU, UK. Tel.: +44 191 222 6422; fax: +44 191 222 6502.

*E-mail address:* [p.d.gosling@ncl.ac.uk](mailto:p.d.gosling@ncl.ac.uk) (P.D. Gosling).

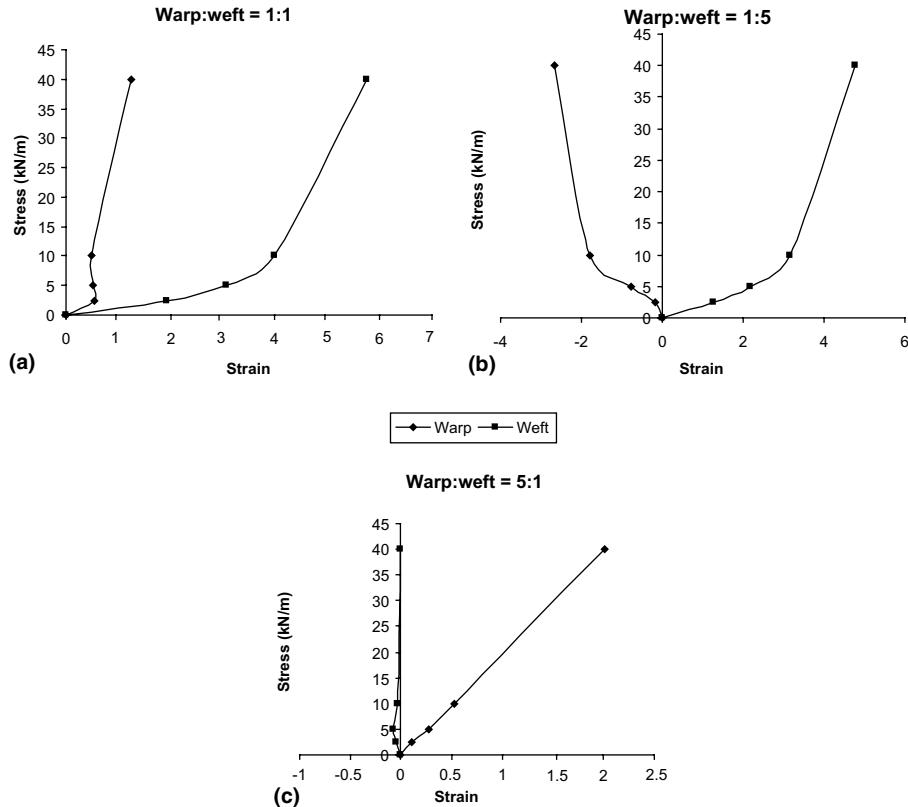


Fig. 1. Biaxial stress–strain curves for PTFE fabric [4].

due to the material properties and frictional effects (inter-fibre and inter-yarn friction). Typical stress–strain curves for PTFE fabric tested at warp to weft stress ratios of 5:1, 1:1 and 1:5 are reproduced from the work of Day [4] in Fig. 1a. These graphs show the key features of the fabric response: sudden changes in gradient (a and c), gradient reversal (i.e. multiple values of stress for a given strain) (a) and negative strain (b and c). These characteristics cause difficulties in establishing a single function which can fit all of the data and be developed into a response surface.

Fabric response varies between batches of fabric and even across the width of a single roll of fabric. The weave pattern is changed by tension varying during weaving and coating. Gripping of the edge of the fabric to move it through the loom causes bowing of the weft yarns. The exact temperature used to sinter PTFE coating on to glass fibre fabric affects the shape of the glass fibres and the level of bond between them at intersections. These variations in fabric behaviour cause further difficulties in describing the behaviour using a single function.

This paper describes two different concepts for the representation of fabric biaxial behaviour:

- (1) The use of Bézier functions, B-splines and NURBS (Non-uniform Rational B-Splines) to define surfaces relating in-plane stresses and strains. Whilst other response surface representations may be adopted (including function derivation using genetic programming [5,6], function parameter optimisation using neural networks [7,8], and response surface methodology [9,10]), spline functions provide an intrinsic interpretation of the test data.
- (2) The pioneering work of Day [4] in which mean stresses and strains are related to stress and strain differences to formulate equations describing fabric biaxial behaviour. This approach is extended and its utility at interpolation between known stress states is investigated.

## 2. Context

### 2.1. Industry perspective

Biaxial tensile tests are carried out on coated woven fabrics at several warp to weft stress ratios to determine the response of the fabric for structural design. Application of the test data in determining material response is typically set within a plane stress framework by:

- (1) Linear interpolation of strains between areas of the structure at known (tested) stress ratios.
- (2) Use of elastic constants (two Youngs’s moduli and one Poisson’s ratio) determined from the secant moduli of warp and weft stress–strain curves at a stress ratio and magnitude deemed typical for the structure. These values remain constant throughout the structural analysis.
- (3) Representation with an elasticity matrix, the general form for two-dimensional anisotropic plane stress involves nine coefficients [3]

$$[D] = \begin{bmatrix} d_{11} & d_{12} & d_{13} \\ d_{21} & d_{22} & d_{23} \\ d_{21} & d_{22} & d_{23} \end{bmatrix}, \quad (1)$$

six of which are independent. With orthogonal weave directions orthotropy can be assumed, hence  $d_{13} = d_{31} = d_{23} = d_{32} = 0$ , leaving four independent variables.

- (4) Use of elastic and interaction moduli,

$$\begin{bmatrix} \sigma_{11} \\ \sigma_{22} \end{bmatrix} = \begin{bmatrix} E_{1111} & E_{1122} \\ E_{1122} & E_{2222} \end{bmatrix} \begin{bmatrix} \varepsilon_{11} \\ \varepsilon_{22} \end{bmatrix}, \quad (2)$$

where  $\sigma$ =stress,  $\varepsilon$ =strain,  $E$ = elastic modulus or stiffness, subscript 11 denotes the warp direction and subscript 22 denotes the weft direction.  $E_{1111}$  is the stiffness in the warp direction,  $E_{1122}$  is the stiffness interaction between warp and weft. Two Poisson’s ratios are defined,

$$\nu_{12} = \frac{E_{1122}}{E_{1111}}, \quad (3)$$

$$\nu_{21} = \frac{E_{1122}}{E_{2222}}, \quad (4)$$

for warp–weft and weft–warp interaction, respectively. Stresses and strains are replaced by small increments  $\Delta\sigma$  and  $\Delta\varepsilon$  to linearise an interval of the non-linear stress–strain curve [11].

For example the three moduli ( $E_{1111}$ ,  $E_{1122}$ ,  $E_{2222}$ ) can be determined between an assumed prestress and an upper value. Incremental loading (both positive and negative) is used to simulate different environmental loads (e.g. wind and snow) and elas-

tic moduli are assessed at different stages of the load history. However, in undertaking tests in two orthogonal directions two values of  $E_{1122}$  are obtained. Typically these are averaged and reported as a single value.

$$\sigma_{11} = \sigma_{11}^i + E_{1111}\varepsilon_{11} + E_{1122}\varepsilon_{22}, \quad (5)$$

$$\sigma_{11} + \Delta\sigma_{11} = \sigma_{11}^i + E_{1111}(\varepsilon_{11} + \Delta\varepsilon_{11}) + E_{1122}\varepsilon_{22}. \quad (6)$$

From Eqs. (5) and (6) it follows that,

$$E_{1111} = \frac{\Delta\sigma_{11}}{\Delta\varepsilon_{11}}, \quad (7)$$

and combining Eqs. (7) and (5) gives,

$$E_{1122} = \frac{\left(\sigma_{11} - \sigma_{11}^i - \frac{\Delta\sigma_{11}\varepsilon_{11}}{\Delta\varepsilon_{11}}\right)}{\varepsilon_{22}}. \quad (8)$$

Similar expressions are obtained in the orthogonal direction for which  $\varepsilon_{11}$  is held constant whilst  $\sigma_{22}$  and  $\varepsilon_{22}$  are allowed to vary. Hence the independent determination of  $E_{1122}$  from both equations.

Use of elastic moduli and an implied Poisson’s ratio makes complete representation of non-linear fabric behaviour somewhat contrived given no compression constraints and shear lock-up [2,12]. Linearisation of parts of the response provide ‘snapshots’ of fabric behaviour, but are not suitable for computer analysis without interpolation. Both approaches proposed in this paper directly relate biaxial stresses to warp and weft strains and so make no assumption about the state of stress in the fabric.

### 2.2. Academic perspective

Kageyama et al. [13] attempted to use a ‘linearising’ method to describe fabric biaxial response. A bilinear approximation gave some limited degree of fit to the test data, but the ‘change point’ needed to be modified for each stress ratio. Testa and Yu [14] modeled non-linear biaxial fabric response using strain energy functions

$$\varepsilon_{ef} = p_1 A_1 \sigma_f^{p_1-1} + A_3 \sigma_w p^3 + p_4 A_4 \sigma_f^{p_4-1} \sigma_w + A_5 \sigma_w, \quad (9)$$

with a similar expression for  $\varepsilon_{ew}$ , where  $\sigma$ =stress,  $\varepsilon$ =strain, and subscripts are defined as follows: e=elastic part of response, w=warp direction, f=fill (or weft) direction. Nine parameters ( $A_1 \dots A_5$  and  $p_1 \dots p_4$ ) were used to fit this polynomial, but the resultant function did not adequately represent the test data. Chen et al. [15] used a simpler second order polynomial to fit the stress–strain data. This enabled the tensile modulus at a given stress level to be derived easily by differentiation.

However, the second order polynomial fit failed to follow discontinuities in the test data.

Lucas [16] developed a technique to fit the non-linear stress–strain curves of PET (polyethylene terephthalate) industrial yarns. The stress–strain curve was converted into a *modulus*–strain curve to exaggerate non-linearities, giving distinct peaks rather than subtle changes in gradient. Three modified Pearson VII lines (or ‘Pearson–Pisa’ lines) were used to fit the modulus–strain curve. This technique was successfully used by Zimlik et al. [17] to fit a function to the non-linear load–extension curves of Teijin filaments. However, the derivation of the modulus–strain curve involved calculation of the gradient of the stress–strain curve by fitting polynomials to a small moving window of data. With widely spaced data points this polynomial fitting would become problematic.

Polynomial representations of fabric tensile stress–strain curves do not sufficiently match the fabric response. In particular they tend to smooth rapid changes in gradient. Bézier curves, B-splines and NURBS [18] can be used to represent curves with rapid changes in gradient or discontinuities. Gradient reversal (Fig. 1a) cannot be represented by a standard polynomial. Spline functions are parametric and hence this feature can be represented easily.

Many curve fitting techniques can be extended to create surface fits to data with three variables, from simple linear interpolation through polynomial fitting to complex spline formulations. Surfaces can be formed by a summation of, for example,  $y, z$  curves in the  $x$  direction, or a grid of intersecting  $y, z$  and  $x, z$  curves. Any surface fit is therefore reliant on good quality curve fitting. The best fit is usually achieved by minimisation of the squared error of the curve/surface fit from the data set.

Minami et al. [19] used response surfaces to represent biaxial fabric behaviour. Orthogonal stresses ( $\sigma_x, \sigma_y$ )<sup>1</sup> and strains ( $\epsilon_x, \epsilon_y$ ) from biaxial fabric tests form surfaces in the  $\sigma_x, \sigma_y, \epsilon_x$  and  $\sigma_x, \sigma_y, \epsilon_y$  coordinate systems. The response surfaces shown in Fig. 2 use results for stress ratios 0:1, 1:1, 2:1, 1:2, 1:0. Elastic constants are established using a multi-step linear approximation. The surface is divided into smaller quadrilaterals and for each quadrilateral the elastic constants are determined. The size of the small quadrilaterals is critical in ensuring discontinuities in the fabric behaviour are accurately captured.

This paper is set in the context of the work of Day [4] in which a fundamentally different approach provides an elegant set of equations to describe fabric response. Average stresses and strains are related to

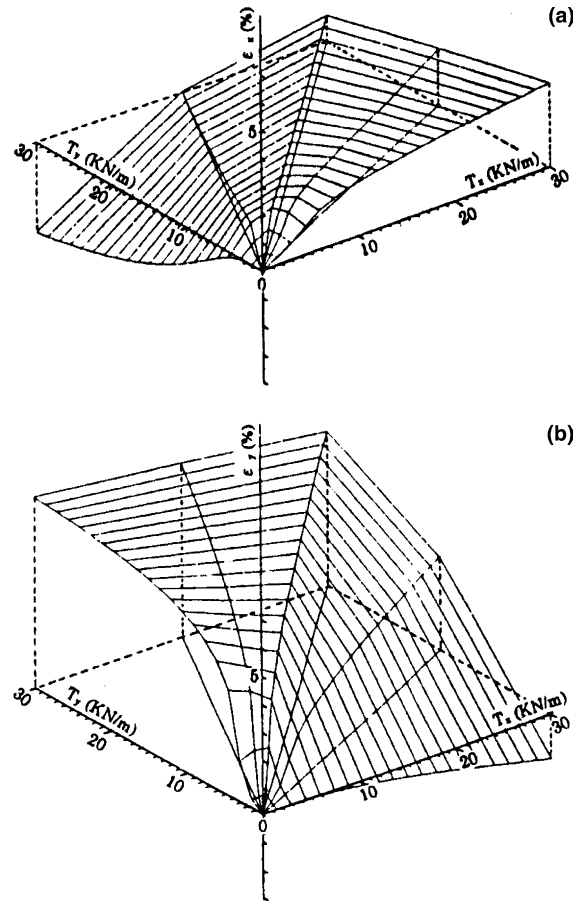


Fig. 2. Biaxial stress–strain response surfaces [19].

differences between warp and weft stresses and strains. An iterative process developed stress–strain relationships applicable to all stress ratios. This was a major step as it attempted to encapsulate the data for three different stress ratios in two simultaneous equations. It is also contrary to the universally adopted plane stress approach.

### 3. Bézier curves, B-splines and NURBS

NURBS (Non-Uniform Rational B-Splines) are mathematical functions used for curve and surface definition. They are a development of piece-wise Bézier curves, known as B-splines. This paper considers the use of all three curve types for response surface generation. NURBS are used as the basis for surface definition in a range of three dimensional computer graphics applications (CAD and animation) and computer controlled machining, and for data representation in signal processing applications. The strength of these parametric functions is an ability to describe *any* continuous

<sup>1</sup>  $x$  and  $y$  denote warp and weft directions, respectively, throughout.

curve or surface with a smooth function whilst allowing local modification of the surface.

3.1. Bézier curves and surfaces

A Bézier curve [20] of degree  $n$  is defined by

$$C(u) = \sum_{i=0}^n B_{i,n}(u)P_i \quad 0 < u \leq 1. \tag{10}$$

The geometric coefficients  $P_i$  are called *control points*. The basis functions  $B_{i,n}$  are the  $n$ th-degree Bernstein polynomials given by

$$B_{i,n}(u) = \frac{n!}{i!(n-i)!} u^i (1-u)^{n-i}. \tag{11}$$

To give greater control over the shape of the curve *control point weighting* can be introduced. This is achieved by modifying the Bézier curve function to a rational function (ie the ratio of two polynomials)

$$C(u) = \frac{\sum_{i=0}^n B_{i,n}(u)w_i P_i}{\sum_{i=0}^n B_{i,n}(u)w_i} \quad 0 < u \leq 1, \tag{12}$$

where  $w_i$  are scalar “weights”. The higher the control point weighting the more it ‘attracts’ the curve (Fig. 3). Bézier functions can be used to define surfaces uses a double summation in two orthogonal directions. A non-rational Bézier surface is defined as

$$S(u, v) = \sum_{i=0}^n \left[ \sum_{j=0}^m B_{i,n}(u)B_{j,m}(v)P_{i,j} \right] \quad 0 < u, v \leq 1, \tag{13}$$

where  $B_{j,m}$  are Bernstein polynomials of the same form as  $B_{i,n}$ . Exactly as before this function can be rewritten as a ratio of two polynomials with control point weighting introduced to give a rational Bézier surface

$$S(u, v) = \frac{\sum_{i=0}^n \left[ \sum_{j=0}^m B_{i,n}(u)B_{j,m}(v)w_i P_{i,j} \right]}{\sum_{i=0}^n \left[ \sum_{j=0}^m B_{i,n}(u)B_{j,m}(v)w_i \right]} \quad 0 < u, v \leq 1. \tag{14}$$

3.2. B-splines

For more complex discontinuous curves a B-spline (a piecewise Bézier curve) is defined [18,20]

$$C(u) = \sum_{i=0}^n N_{i,p} P_i \quad a \leq u \leq b. \tag{15}$$

The B-spline basis functions  $N_{i,p}$  can be defined in several ways; as divided differences of truncated power functions, and using blossoming and recurrence formula. Recurrence tends to be used since it is well suited to computer implementation. A B-spline basis function of  $p$ -degree is defined recursively as

$$N_{i,0}(u) = 1 \text{ if } u_i \leq u < u_{i+1} \\ = 0 \text{ otherwise} \tag{16}$$

$$N_{i,p}(u) = \frac{u - u_i}{u_{i+p} - u_i} N_{i,p-1}(u) + \frac{u_{i+p+1} - u}{u_{i+p+1} - u_{i+1}} N_{i+1,p-1}(u). \tag{17}$$

The B-spline has breakpoints called knots. The knot vector  $U$  is an ascending sequence

$$U = (u_0, \dots, u_m). \tag{18}$$

A simple B-spline has a uniform, periodic knot vector  $U = (1, 2, 3, \dots, p)$ . However, non-periodic, non-uniform, knot vectors allow more control of the shape of the curve

$$U = (\underbrace{a, \dots, a}_{p+1 \text{ terms}}, u_{p+1}, \dots, u_{m-p+1}, \underbrace{b, \dots, b}_{p+1 \text{ terms}}). \tag{19}$$

For example coincident knots can be used to specify end conditions and facilitate the introduction of discontinuities.

3.3. NURBS

NURBS [21,22], are Non-Uniform Rational B-Splines; B-splines with non-uniform knot vectors expressed as a ratio of two functions. The non-uniform

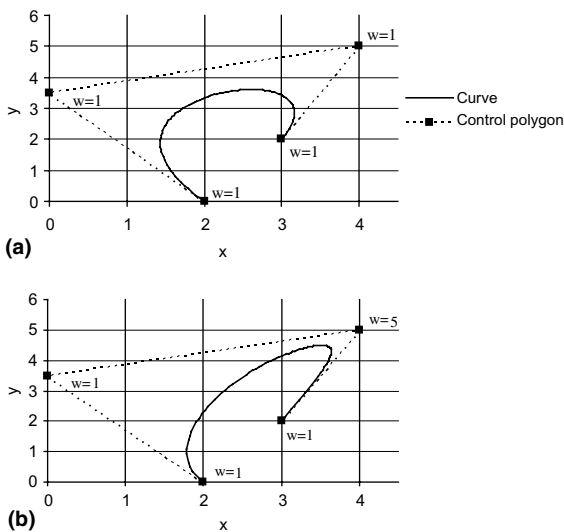


Fig. 3. Effect of control point weighting on Bézier curve.

B-spline (Eqs. (15)–(19)) is modified in the same way as the Bézier function—a rational function is formed to facilitate the introduction of *control point weighting*

$$C(u) = \frac{\sum_{i=0}^n N_{i,p}(u)w_iP_i}{\sum_{i=0}^n N_{i,p}(u)w_i} \quad a \leq u \leq b. \quad (20)$$

Control point weighting gives further local control over curve shape. With modification of control point locations and weights a broad range of curves can be defined. Finally the NURBS curve can be summed in a third dimension to give a NURBS surface. The knot vector becomes a two-dimensional *control net*:

$$S(u, v) = \frac{\sum_{i=0}^n \sum_{j=0}^m w_{i,j}N_{i,p}(u)N_{j,q}(v)P_{i,j}}{\sum_{i=0}^n \sum_{j=0}^m w_{i,j}N_{i,p}(u)N_{j,q}(v)}, \quad (21)$$

where  $u, v$  are parameters,  $N_{i,p}, N_{j,q}$  are basis functions,  $P_{i,j}$  are control points,  $w_{i,j}$  are control point weights and  $U, V$  are knot vectors.

It is interesting to note that this summation can be continued to any number of dimensions. The resulting function becomes difficult to visualise, but can potentially be used to describe the relationship between any number of independent variables with non-linear relationships. For example, to relate four variables a summation of NURBS surfaces could be used (a NURBS solid)

$$S(u, v, w) = \frac{\sum_{i=0}^n \sum_{j=0}^m \sum_{k=0}^l w_{i,j,k}N_{i,p}(u)N_{j,q}(v)N_{k,r}(w)P_{i,j,k}}{\sum_{i=0}^n \sum_{j=0}^m \sum_{k=0}^l w_{i,j,k}N_{i,p}(u)N_{j,q}(v)N_{k,r}(w)}. \quad (22)$$

This extension to multivariate representation can equally be applied to Bézier and B-spline functions.

### 3.4. Response surface generation for fabric test data

The following response curve and surface generation is based on data from the work of Day [4]. Surfaces generated using Bézier and spline functions are essentially summations of many curves. It is therefore useful to assess a function’s capability for representation of non-linear biaxial test curves before attempting to develop a response surface. A suitable combination of control point locations and weights fits a single Bézier curve to non-linear data points with multiple gradient reversals (e.g. Fig. 4, data from Fig. 1a, ‘warp curve’).

For more contorted test data the number of control points can be increased until all data are successfully

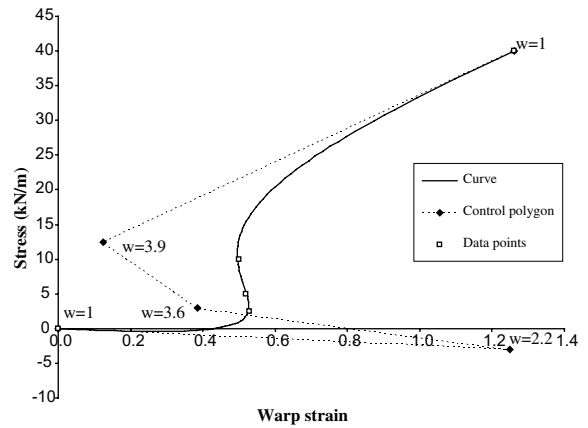


Fig. 4. Data fitting using rational Bézier curve.

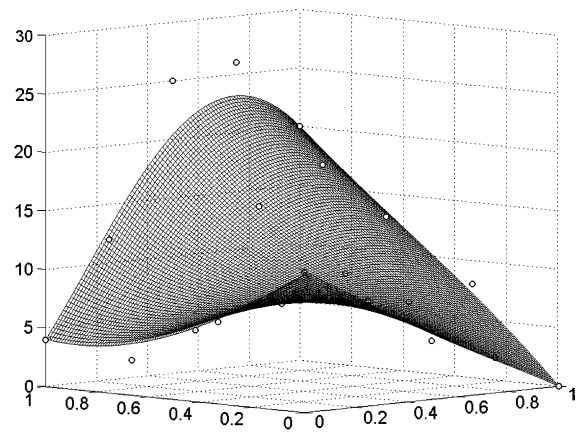


Fig. 5. Rational Bézier surface defined by 20 control points.

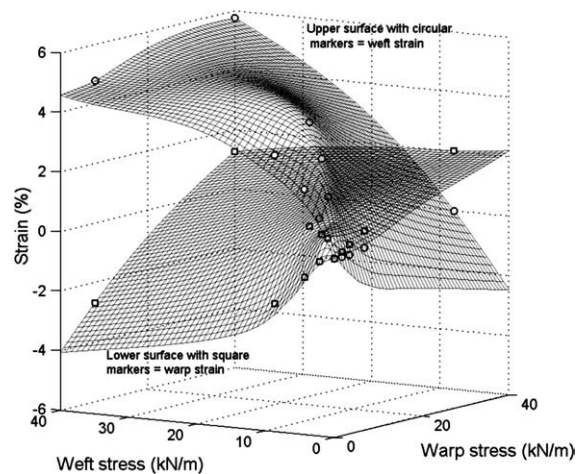


Fig. 6. Warp and weft response surfaces.

interpolated. The same procedure can be used to fit a surface to data with three variables. To simplify calculation a regular grid of control points is used (a *control net*) and the location of control points is only modified in the  $z$  direction. The control point weights can also be varied (Fig. 5). It is important to note that the circular points shown are the control net and *not* the data points. The data points would lie on the surface once optimisation had been carried out [In Fig. 5 no data points are shown].

Bézier surfaces are defined by continuous functions with easily obtainable derivatives, making them highly suitable for inclusion in finite element structural analysis software. Two surfaces are required to describe fabric behaviour under biaxial tensile stress; one for warp strain and one for weft strain (Fig. 6).

Use of NURBS functions gives greater control over the curve or surface shape. In particular, the non-uniform knot vector allows discontinuities in the response to be included. This is required if the fabric stress–strain response is discontinuous; if the change in curvature is rapid but not instantaneous then a Bézier representation will suffice. Discontinuities in the response surface are undesirable for non-linear finite element analysis as they could lead to numerical instabilities.

#### 4. Pioneering work of Day [4]

Day’s [4] work is based on the representation of non-linear stress–strain behaviour in soil mechanics [23] in which the mean and difference of the principal strains are related. Because fabric shear stiffness is low the material can be treated as orthotropic. Hence the principal stresses lie in warp and weft directions and the shear stresses can be dealt with separately, such that,

$$\sigma_a = \frac{(\sigma_x + \sigma_y)}{2}, \tag{23}$$

$$\epsilon_a = \frac{(\epsilon_x + \epsilon_y)}{2}, \tag{24}$$

$$T = \frac{(\sigma_y - \sigma_x)}{2}, \tag{25}$$

$$g = \frac{(\epsilon_x - \epsilon_y)}{2}, \tag{26}$$

$$\sigma_a = f^1(\epsilon_a) + f^2(g), \tag{27}$$

$$T = f^3(\epsilon_a) + f^4(g), \tag{28}$$

where  $\sigma_x$ =warp stress,  $\sigma_y$ =weft stress,  $\sigma_{xy}$ =shear stress,  $\epsilon_x$ =warp strain,  $\epsilon_y$ =weft strain,  $\epsilon_{xy}$ =shear strain and  $f^1$  to  $f^4$  are functions to be determined. Shear stress and

strain are related by an independent linear function  $f^5$  [4],

$$\sigma_{xy} = f^5(\epsilon_{xy}). \tag{29}$$

Discontinuities in the test results made reproduction of the curves impossible using algebraic functions (e.g. polynomials) for  $f^1$  to  $f^4$  [4]. Therefore ‘arbitrary’ stress–strain curves have been defined by a set of points with linear interpolation. This leaves a non-linear curve fitting problem if a differentiable function is required to predict a tangent modulus under a plane stress assumption.

##### 4.1. Application to fabric test data

In this paper both polynomials and arbitrary points with linear interpolation have been used for functions  $f^1$  to  $f^4$ . Day’s [4] original test data have been used (Fig. 1 and Table 1). Because of the interaction between terms in the four functions, direct derivation is not possible and an iterative approach is required [4]. The starting point is the determination of  $f^1$  in Eq. (27). For a biaxial stress ratio of 1:1, the stress difference ( $g$ ) is zero, hence,

$$\sigma_a = f^1(\epsilon_a) \text{ for } 1 : 1 \text{ stress ratio.} \tag{30}$$

Values for mean stress ( $\sigma_a$ , equals applied stress for 1:1 stress ratio) and mean strain ( $\epsilon_a$ ) can be taken from the 1:1 warp and weft curves (Fig. 1a and Table 1), giving a first approximation to  $f^1$ . Fig. 7 shows the data points used to define  $f^1$  fitted with both linear interpolation and a fourth order polynomial. A similar process is used to determine the relationship

$$T = f^3(\epsilon_a), \tag{31}$$

again using the 1:1 test data [4]. This is difficult to follow as  $T$  (stress difference) is, by definition, zero for a 1:1 stress ratio. Day considers what the stress difference would be if the warp and weft strains were equal and set to a given value. In this paper it is argued that for a 1:1 stress ratio it is implicit that the stress difference is zero and hence  $f^3(g)$  must be zero for all values of  $T$ .<sup>2</sup>

The functions  $f^2(g)$  and  $f^4(g)$  are obtained using data from the 5:1 and 1:5 test curves (Fig. 1b and c and Table 1). The following example is taken from Day’s paper [4].<sup>3</sup>

<sup>2</sup> Day’s method of determining  $f^3$  was carried out, but the resultant curve fits were poor compared to those achieved with  $f^3(\epsilon_a)=0$ .

<sup>3</sup> The notation has been modified in line with this paper, and some corrections have been made to signs and significant figures.

Table 1  
Test data and determination of functions [4]

Stress ratio	$\sigma_x$ (kN/m)	$\sigma_y$ (kN/m)	$\varepsilon_x$ (%)	$\varepsilon_y$ (%)	$\sigma_a$ (kN/m)	$T$ (kN/m)	$\varepsilon_a$ (%)	$g$ (%)	Values of $\sigma_a$ from $f_1(\varepsilon_a)$ (kN/m)	Values for $f_2(g)$ ( $f_2(g) = \sigma_a - f_1(\varepsilon_a)$ ) (kN/m)
1:1	0	0	0	0	0	0	0	0	–	–
1:1	2.5	2.5	0.53	1.93	2.5	0	0.0123	–0.007	–	–
1:1	5	5	0.52	3.06	5	0	0.0179	–0.0127	–	–
1:1	10	10	0.5	3.99	10	0	0.0225	–0.0175	–	–
1:1	40	40	1.26	5.74	40	0	0.035	–0.0224	–	–
5:1	0	0	0	0	0	0	0	0	0.00	0.00
5:1	2.5	0.5	0.11	–0.05	1.5	–1	0.0003	0.0008	0.23	1.27
5:1	5	1	0.27	–0.08	3	–2	0.001	0.00175	0.66	2.34
5:1	10	2	0.53	–0.04	6	–4	0.0025	0.00285	1.39	4.61
5:1	40	8	2.01	–0.01	24	–16	0.01	0.0101	2.34	21.66
1:5	0	0	0	0	0	0	0	0	0.00	0.00
1:5	0.5	2.5	–0.17	1.27	1.5	1	0.0055	–0.0072	2.07	–0.57
1:5	1	5	–0.78	2.17	3	2	0.007	–0.0148	2.18	0.82
1:5	2	10	–1.8	3.17	6	4	0.0069	–0.0249	2.17	3.83
1:5	8	40	–2.67	4.77	24	16	0.0105	–0.0372	2.39	21.61

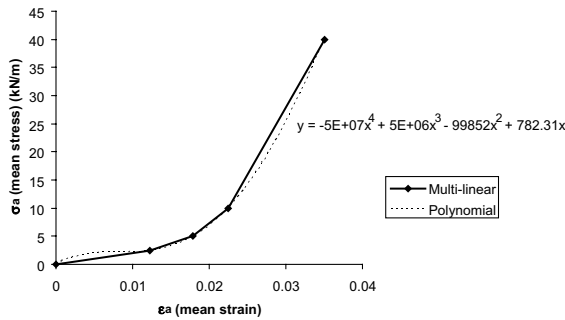


Fig. 7. Function  $f^1$  from 1:1 test data.

Consider the 5:1 curve: at  $\sigma_x = 10$  kN/m,  $\sigma_y = 2$  kN/m,  $\varepsilon_x = -0.0004$  and  $\varepsilon_y = 0.0053$ . Then

$$\sigma_a = \frac{(\sigma_x + \sigma_y)}{2} = 6 \text{ kN/m} = \sigma'_a \quad (32)$$

$$\varepsilon_a = \frac{(\varepsilon_x + \varepsilon_y)}{2} = 0.0023, \quad (33)$$

$$T = \frac{(\sigma_y - \sigma_x)}{2} = -4 \text{ kN/m}, \quad (34)$$

$$g = \frac{(\varepsilon_x - \varepsilon_y)}{2} = 0.0027. \quad (35)$$

For this value of  $\varepsilon_a$  there will be a value of  $\sigma_a$  from  $\sigma_a = f^1(\varepsilon_a)$ . Using the polynomial fit to  $f^1$  (Fig. 7) gives  $\sigma_a = 1.39$  kN/m (not 6 as given by Eq. (32)). This difference between  $\sigma_a$  and  $\sigma'_a$  provides data for the function

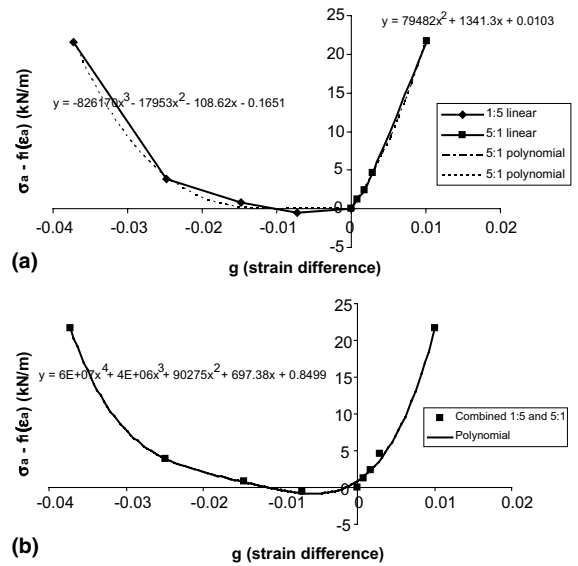
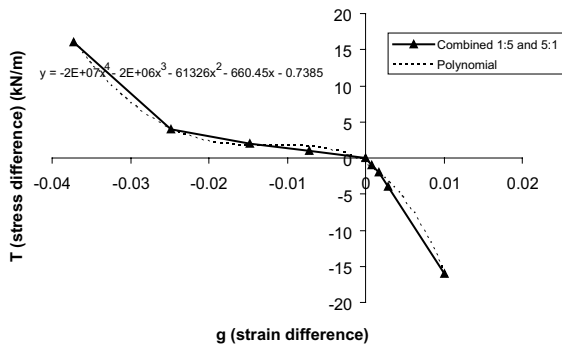


Fig. 8. Function  $f^2$ .

$f^2$ . Fig. 8 shows several curve fits to the  $f^2$  data: in 8a the data has been linearly interpolated and fit with a two part second order polynomial, 8b shows a single fourth order polynomial. Determination of  $f^4$  is simplified by the fact that  $f^3 = 0$ , hence:

$$T = f^4(g). \quad (36)$$

This function can be determined directly from the 1:5 and 5:1 data, and is shown in Fig. 9 with linear interpolation between points and with a fourth order poly-

Fig. 9. Function  $f^4$ .

mial. Day's original results, and the values used to determine functions  $f^1$  to  $f^4$  are given in Table 1. A unit square of fabric was simulated, subjected to biaxial stresses with the stress–strain behaviour of the element determined by his stress–strain mean-difference functions [4]. An iterative process allowed the arbitrary curves defining functions  $f^1$  to  $f^4$  to be modified to minimise the discrepancies between the computer prediction and test results. The results following this iterative process are shown in Fig. 10. Without any iterative modification of the functions shown in Figs. 7–9 the predicted response compares well with the test results, in particular for the polynomial functions where three polynomials are being used to represent six non-linear relationships. Predicted response and original test results are shown in Fig. 11 (based on linear interpolation between values) and Fig. 12 (using polynomial functions). With modification of the multi-linear curves and the polynomial functions (or using different function forms) a very good representation of the original data could be achieved (as seen in Fig. 10). This optimisation has yet to be carried out.

## 5. Quality of response representations

### 5.1. Bézier functions, B-splines and NURBS

#### 5.1.1. A unique solution?

Fig. 4 shows a Bézier curve fit to typical fabric stress–strain data. The ability to fit these data points which cannot be readily represented by a polynomial demonstrates the utility of Bézier curves. A different curve fit to identical data using the same Bézier function can be obtained (Fig. 13, 'Curve 2' defined by 'Control polygon 2'). This has been superimposed on the previous curve (from Fig. 4) which is labelled 'Curve 1'. [Note that points a and e are data points and are also the end points of both control polygons, and all control points at these locations have a weight of 1]. Two combinations of control point locations and weights give equally valid curves

which interpolate the data set (Fig. 13). Both curves have been fit by trial and error, but a simple routine to minimise the mean square offset from the data points would achieve an exact fit. By varying control point locations and weights a large family of interpolating curves can be generated. All of these curves have a mean square offset from the data of zero. Hence an optimisation routine based solely on this criterion would not be able to distinguish between them. The differences between these interpolating functions can be significant (Fig. 13). The deviation of the curves between points *d* and *e* clearly demonstrates this difference, highlighting that the response surfaces in Fig. 6 do not provide a reliable model of fabric behaviour. They are arbitrary surfaces that interpolate the data points. Further data is required to establish which curve or surface best represents the fabric response. However, with additional data the same uncertainty will occur between data points, albeit on a smaller scale. This non-uniqueness relative to a fixed data set is a fundamental problem with Bézier curves, B-splines and NURBS in their basic form. These functions are useful for generating a smooth, differentiable function that interpolates the data, but additional criteria are required to optimise the fit between data points.

In addition to minimisation of the square of the mean error, a combination of two further criteria (and specification of a weighting parameter) would achieve a unique fit: minimisation of the deviation of the curve from the straight line joining consecutive points and minimisation of the rate of change of curvature. A single parameter would provide the weighting attributed to these two conditions. To avoid the need for calibration tests to determine this parameter more advanced optimisation methods could be used. For example, the gradient (and rate of change of gradient) of a polynomial fit to a moving window of data could be used as a basis for the gradient of the interpolating Bézier function. However, with widely spaced non-linear data this polynomial fit could present difficulties.

#### 5.1.2. Discontinuity and local control

In computer graphics applications the NURBS non-uniform knot vector is utilised to model discontinuities (to define sharp edges) and hence to facilitate detailed local control of the surface shape. Fabric stress–strain curves are described as 'discontinuous' in that they have distinct non-linearities (Fig. 1) and hence are difficult to model with a polynomial function [14,15]. A NURBS representation is required if these non-linearities include an instantaneous change in curvature. Available data from literature [4,14,15,12,24], and from industry either suggest that the stress–strain curves are continuous, or give too few points to make an assessment. For typical engineering materials (e.g. steel) there are no discontinuities in the stress–strain curve until failure. However the

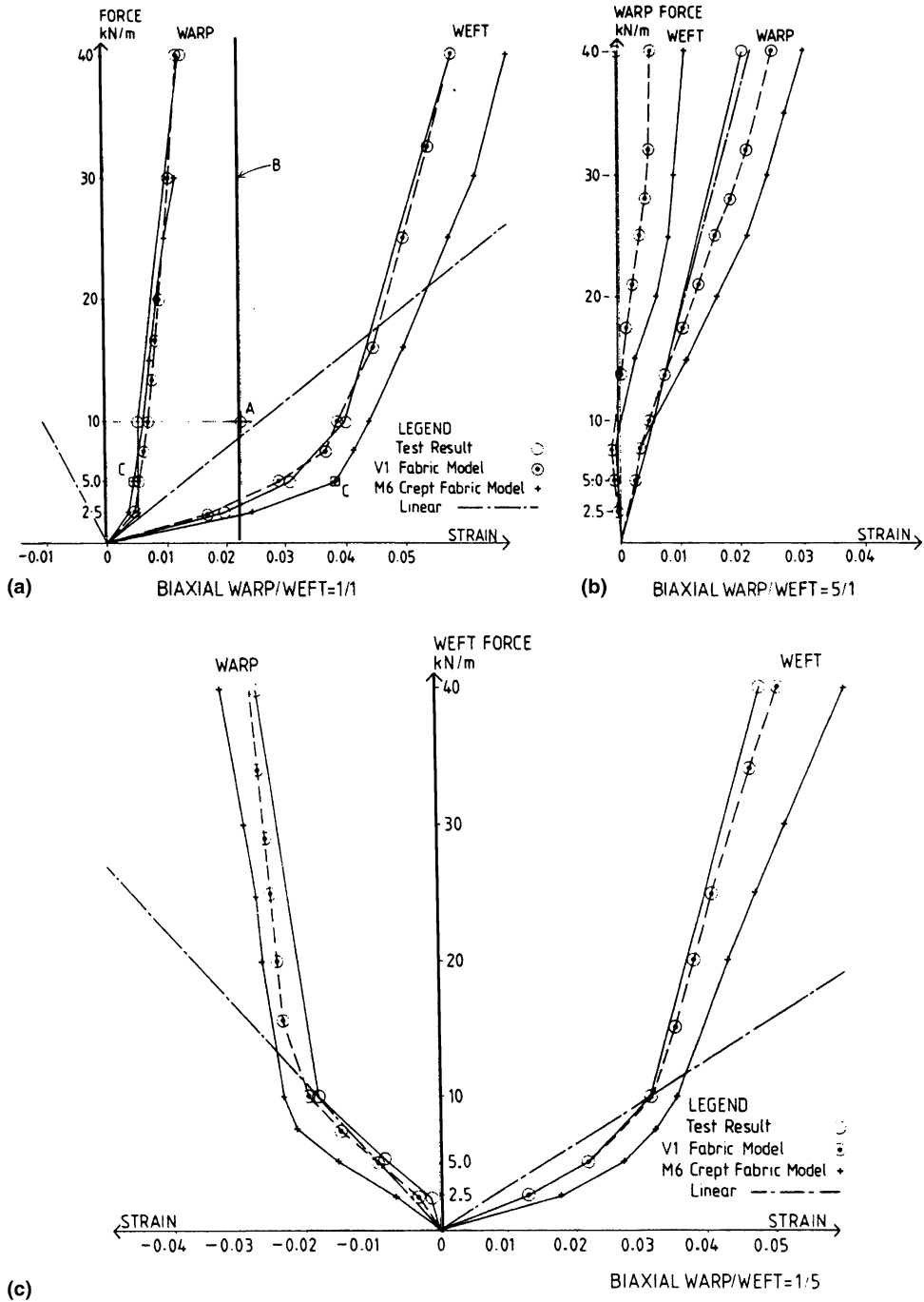


Fig. 10. Day's results and prediction from model [4].

deformation mechanism of woven fabrics under biaxial load are complex and geometric effects could lead to discontinuity.

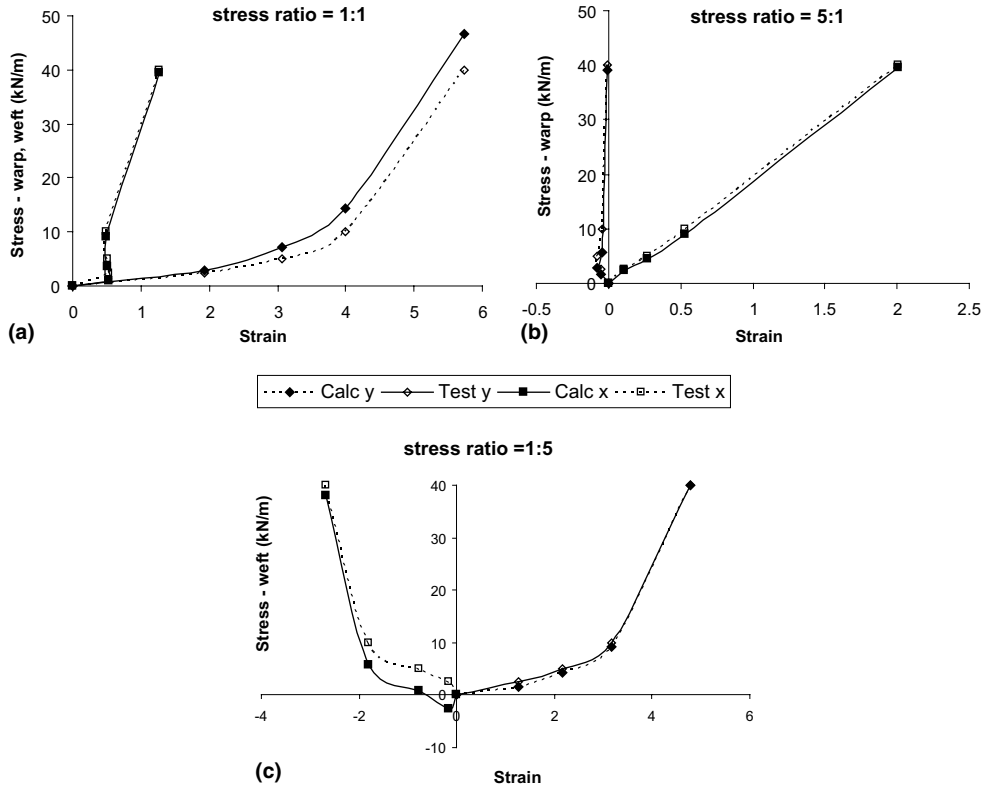


Fig. 11. Response predicted using linearly interpolated functions.

## 5.2. Day's method [4]

### 5.2.1. Analysis of mean and difference functions

It is useful to understand why the three functions  $f^1$ ,  $f^2$  and  $f^4$  produce reasonably good curve fits to the test data. For example, in,

$$\sigma_a = f^1(\epsilon_a) + f^2(g),$$

at a stress ratio of 1:1  $f^1(\epsilon_a)$  is large compared to  $f^2(g)$  and therefore  $f^1(\epsilon_a)$  dominates the response. This gives a good curve fit as  $f^1(\epsilon_a)$  was determined from 1:1 test data. For 1:5 and 5:1 ratios  $f^1(\epsilon_a)$  is small compared to  $f^2(g)$  and hence  $f^2(g)$  dominates the response. Again a good fit is achieved as  $f^2(g)$  was determined from 1:5 and 5:1 test data.

Furthermore, it has been noted with respect to,

$$T = f^3(\epsilon_a) + f^4(g),$$

that  $f^3(\epsilon_a)$  must equal zero for a stress ratio of 1:1. This leaves  $T = f^4(g)$ . For a stress ratio of 1:1,  $f^4(g)$  is small compared to  $\sigma_a$ . This provides a good fit as  $f^4(g) = 0$  (hence  $T = \text{stress difference} = 0$ ) would give the best fit to the 1:1 curve. For the 1:5 and 5:1 ratios  $f^4(g)$  is determined from the relevant test data, and so achieves a good fit to the test curves.

### 5.2.2. Prediction of stress–strain behaviour for intermediate stress ratios

For Day's stress–strain mean and difference functions [4] to be suitable for the representation of fabric behaviour they must successfully predict the fabric strains for stress ratios other than those tested. Day's work makes no mention of how well intermediate stress states are predicted, or how stable the functions are in these areas.

In the absence of additional test data, stress–strain curves for stress ratios of 2:5 and 5:2 have been derived by linear interpolation between the 1:5, 5:1 and 5:1 test data with the aim of further defining the response functions. These 2:5 and 5:2 curves are not expected to accurately represent the fabric behaviour, but they do represent a *feasible* response which can be used to test the validity of Day's method. Fig. 14 shows values of  $\sigma_a$  and  $g$  ( $= \text{strain difference} / 2$ ) for stress ratios 1:5, 2:5, 5:2 and 5:1.

These four curves cannot be encapsulated in a single function, as was possible for the 1:5 and 5:1 curves. Rather than further defining a single curve, test data for additional stress ratios provide a scatter of points (Fig. 14). Consideration of the physical meaning of  $\sigma_a$  and  $g$  suggests that this data scattering is fundamental and not due solely to the linearly interpolated 2:5 and 5:2 curves. For example equal strains in both warp

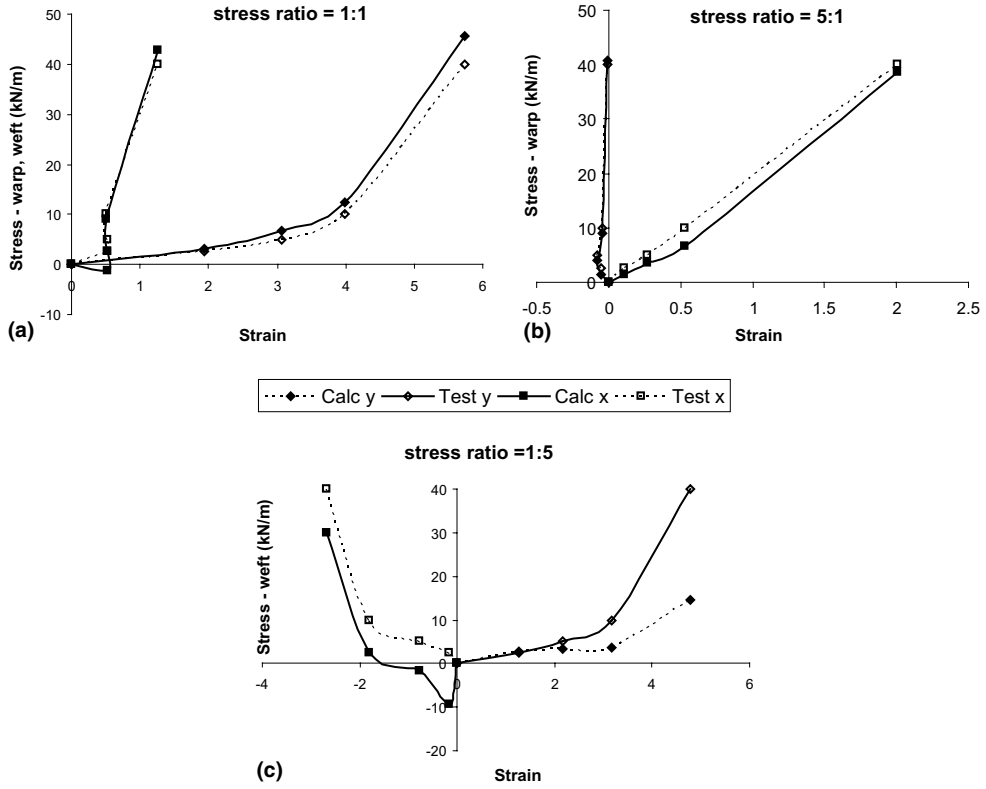


Fig. 12. Response predicted using polynomial functions.

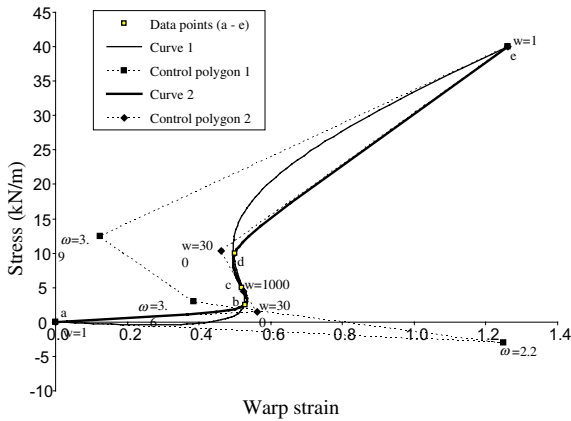


Fig. 13. Data fitting using rational Bézier curve—another solution.

and weft directions (i.e.  $g=0$ ) could be achieved with numerous pairs of applied stresses. This would give many values of mean stress ( $\sigma_a$ ) which will all lie on the vertical axis. Similarly other stress states will populate the graph in Fig. 14 with a scatter of points.

The behaviour of the response functions  $f^1, f^2$  and  $f^4$  at intermediate stress ratios can be examined by plotting

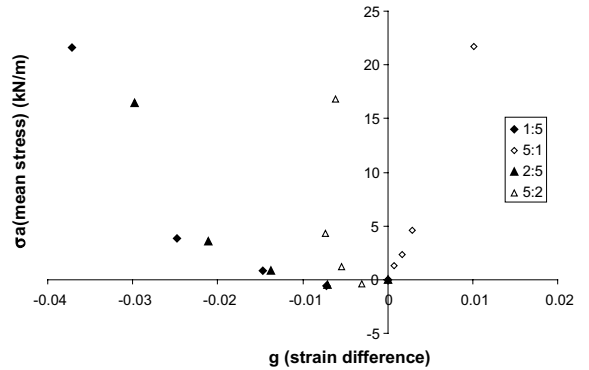


Fig. 14. Definition of  $f^2(g)$  using four stress ratios.

surfaces defined by Eqs. (27) and (28). Figs. 15 and 16 show  $\sigma_x, \sigma_y, \epsilon_x$  and  $\sigma_x, \sigma_y, \epsilon_y$  response surfaces respectively. The surface is shown as a cloud of hollow circles, four views of each surface are given to make the shape of the function clear. Test data points are shown by solid circles. The surfaces shown are based on multi-linear response functions, the polynomial functions provide very similar surfaces.

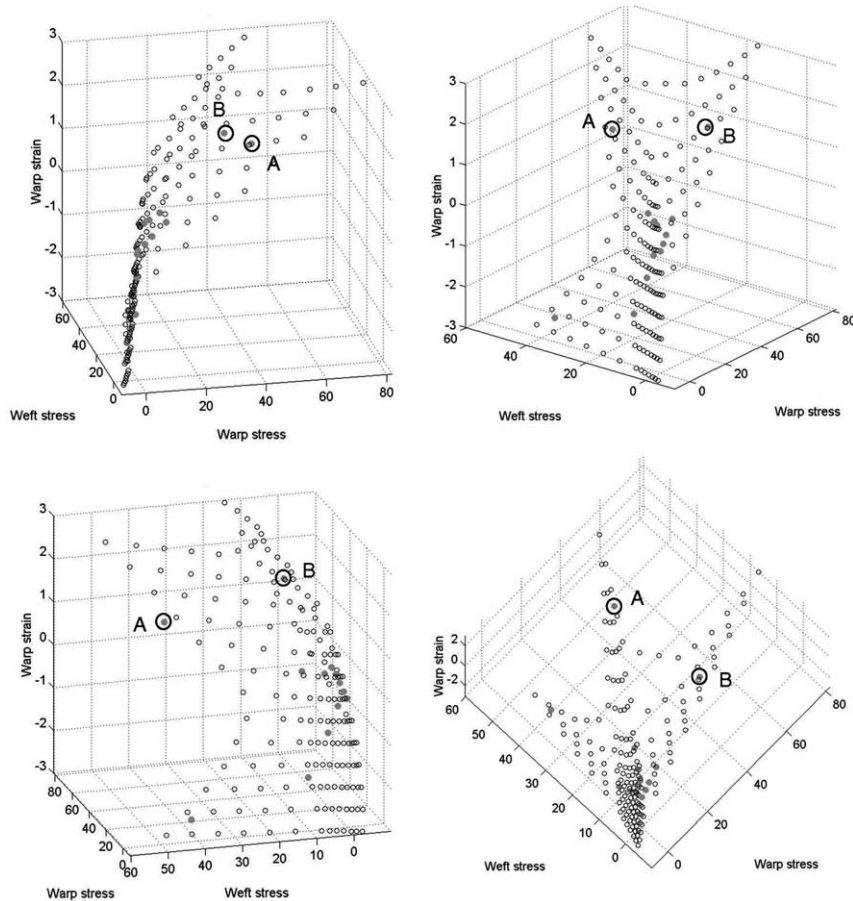


Fig. 15. Warp response surface from mean-difference functions.

These figures show the response surface providing a good fit to all data points, as already seen in Figs. 11 and 12. However, between data points the response surface shape gives highly unpredictable results. Useful comparison can be made with surfaces generated using linear interpolation (Fig. 2) and with an interpolating spline (Fig. 6). Points 'A' and 'B' are data points on the warp surface (Fig. 15)

A:  $\sigma_x = 40$ ,  $\sigma_y = 40$ ,  $\varepsilon_x = 1.26\%$

B:  $\sigma_x = 40$ ,  $\sigma_y = 8$ ,  $\varepsilon_x = 2.01\%$

Point C (not shown) lies between 'A' and 'B':

C:  $\sigma_x = 40$ ,  $\sigma_y = 20$ ,  $\varepsilon_x = ?$

It is reasonable to assume that the value of  $\varepsilon_x$  lies between 1.26% and 2.01%. The value given by the mean and difference response functions shown in Fig. 15 is  $\approx 3.18\%$ .

### 5.3. Incorporation of other aspects of fabric behaviour

Representation of biaxial test data does not fully describe coated woven fabric behaviour. Shear is often ne-

glected, Day [4] assumed shear stiffness was low, uncoupled to stress-strain behaviour, and linear elastic. However a thorough treatment of woven fabric shear behaviour shows it be non-linear, hysteretic and discontinuous [25,26]. The response of coated woven fabrics to biaxial loads is more complex than is shown by Day's results (Fig. 1), which only give the response to initial loading. The following factors are all important in determining the response:

- (1) Load history (mechanically conditioned behaviour achieved by cyclic load regimes differs from initial behaviour).
- (2) Rate of loading.
- (3) Increasing or decreasing load.
- (4) Temperature.
- (5) Creep and relaxation.

Bézier functions and NURBS have potential to be extended to describe test results including any of these factors. All of these factors have a non-linear influence on

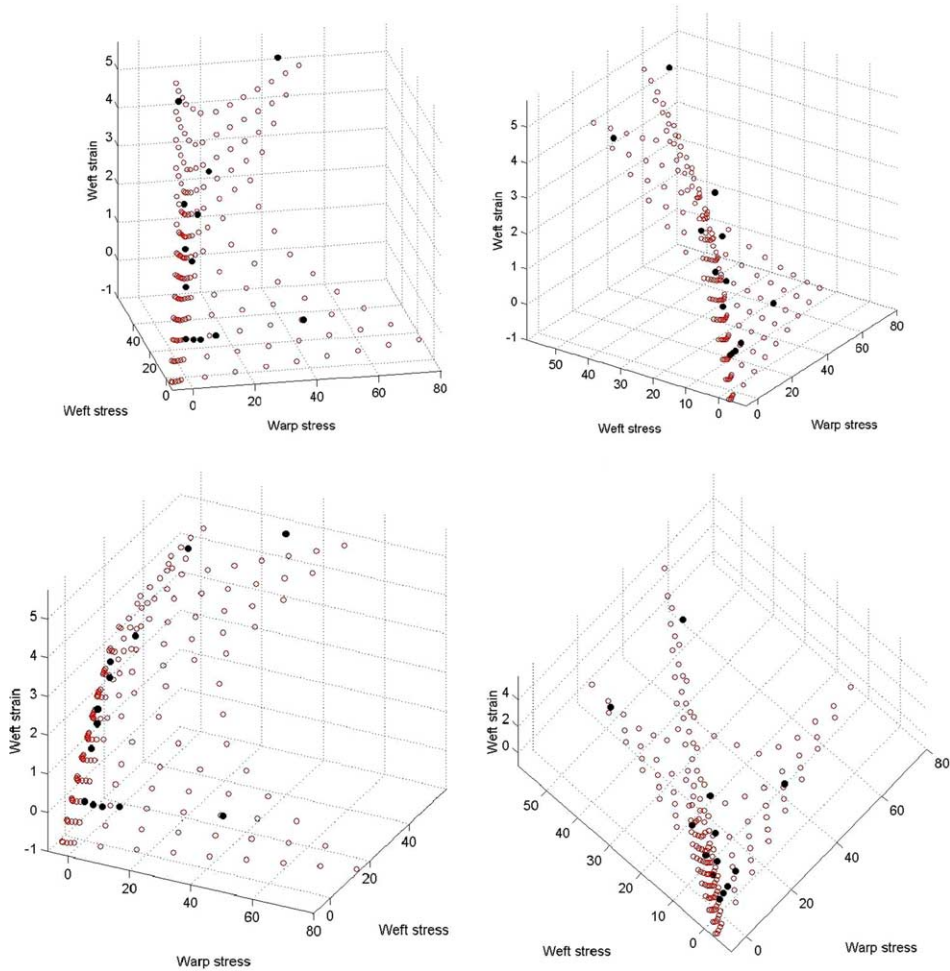


Fig. 16. Weft response surface from mean-difference functions.

fabric behaviour, hence spline functions are well suited to their representation. Variation in shear modulus is discontinuous and so may require NURBS. Eq. (22) shows how NURBS can be extended to describe four independent variables. The summation can be repeated to include any number of independent variables. The response is difficult to visualise, but will provide a single function that describes any number of variables.

Day's [4] methodology of relating stress and strain means and differences is not as readily applied to other factors affecting the response. Further work is proposed on the modification of Day's formulae to include additional variables to account for other aspects affecting fabric response.

Previous work [2–4,13,14,19] has looked at fitting a curve or surface to a single set of fabric biaxial test data. The behaviour of fabric is inherently variable due to various stages of the weaving and coating processes. To fully understand the bounds of the response of a fabric,

multiple tests should be carried out on different batches and with samples taken from different parts of the roll. Upper and lower bounding surfaces could be fit to the resulting scattered data points. These two surfaces could be used for structural analysis—upper or lower bounds used as appropriate to give a conservative design.

## 6. Conclusions and recommendations

Two techniques have been presented in this paper that provide alternatives to plane stress formulations for coated woven fabric behaviour. Both methods directly relate biaxial stresses to warp and weft strains, thus avoiding plane stress assumptions which may not apply to coated woven fabric behaviour.

Response surfaces defined with rational Bézier functions can model data with rapid changes in gradient and multiple gradient reversals (Fig. 6). Multiple optimi-

sation criteria are required to achieve a unique solution (Figs. 4 and 13). NURBS have the same benefits and drawbacks as Bézier functions, with the additional ability to represent discontinuities in the data. Further testing is required to determine whether coated woven fabric stress–strain response exhibits true discontinuities and hence requires B-spline or NURBS representation. Biaxial fabric tests with frequent readings would determine the shape of the stress–strain curve and identify discontinuities. This type of data could also be used for calibration or validation of Bézier function optimisation routines.

Day [4] proposed a novel method of using relationships between stress and strain means and differences to represent fabric biaxial behaviour. This elegant method provides a good fit to non-linear test data for three stress ratios using polynomials or multi-linear functions. Iterative analysis of a simulated test piece and function modification optimise the fit. The use of mean and difference formulae enables six non-linear curves to be described by three polynomial functions. Further biaxial tests need to be undertaken to determine whether more than three stress ratios can be used to further inform the mean and difference functions and to provide evidence that the functions lead to meaningful interpolation between the tested stress states.

#### Acknowledgment

This research is supported by the EPSRC (Engineering and Physical Sciences Research Council, award number 01301420), Arup and Architen-Landrell.

#### References

- [1] Peirce FT. The geometry of cloth structure. *J Textile Inst* 1937;28:81–8.
- [2] Skelton J. Mechanical properties of coated fabrics. In: Hearle J, Thwaites J, Amirbayat J, Rijn A, editors. *Mechanics of Flexible Fibre Assemblies*. Netherlands: Sijthoff & Noordhoff; 1980. p. 461–9.
- [3] Tan KY, Barnes MR. Numerical representation of stress–strain relations for coated fabrics. In: *IstructE symposium on design of air supported structures*, Bristol. 1984. p. 162–74.
- [4] Day AS. Stress strain equations for non-linear behaviour of coated woven fabrics. *IASS symposium proceedings: shells, membranes and space frames*, Osaka, 2. Amsterdam: Elsevier; 1986. p. 17–24.
- [5] Koza JR. *Genetic programming on the programming of computers by means of natural selection*. Cambridge, Massachusetts, USA: The MIT Press; 1992.
- [6] Brunetti A. Fast and precise genetic algorithm for a non-linear fitting problem. *Comput Phys Commun* 2000;124(2–3):204–11.
- [7] Hutchinson A. *Algorithmic learning*. Graduate texts in computer science. Oxford: Clarendon Press; 1994.
- [8] Masters T. *Advanced algorithms for neural networks, a C++ sourcebook*. USA: John Wiley & Sons Inc.; 1995.
- [9] Myers RH. Response surface methodology—current status and future directions. *J Qual Technol* 1998;31(1):30–44.
- [10] Myers RH, Khuri AI, Carter WH. Response surface methodology: 1966–1988. *Technometrics* 1989;31(2):137–57.
- [11] Blum R. Approval for structural membranes proposal TEXT. 14–15, Internet, accessed November 2002. <<http://www.tensinet.com/documents/working/Approval>>.
- [12] Skelton J. The biaxial stress–strain behavior of fabrics for air supported tents. *J Mater* 1971;6(3):656–82.
- [13] Kageyama M, Kawabata S, Niwa M. The validity of a linearizing method for predicting the biaxial-extension properties of fabrics. *J Textile Inst* 1988;79:543–65.
- [14] Testa RB, Yu LM. Stress–strain relation for coated fabrics. *J Eng Mech* 1989;113(11):1361–646.
- [15] Chen Y, Lloyd DW, Harlock SC. Mechanical characteristics of coated fabrics. *J Textile Inst* 1995;86(4):690–700.
- [16] Lucas LJ. Mathematical fitting of modulus–strain curves of PET industrial yarns. *Textile Res J* 1983;53:771–7.
- [17] Zimliki DA, Kennedy JM, Hirt DE, Reese GP. Determining mechanical properties of yarns and two-ply cords from single filament data Part II: comparing model and experimental results for PET. *Textile Res J* 2000;70(12):1097–105.
- [18] Dierckx P. *Curve and surface fitting with splines*. Oxford: Oxford Science Publications, Clarendon Press; 1993.